High-Speed Circuits and QCAs

Circuit configurations:
- Digital applications
  - CMOS
  - E/D-mode logic
  - Current mode logic
- RF applications
  - nFET drivers
  - Resistive, inductive, or active loads

Emerging technologies:
- QCA
- MEMS
- Molecular electronics
- …

IEEE ELECTRON DEVICE LETTERS, VOL. 18, NO. 8, AUGUST 1997

Fabrication and Characterization of an InAlAs/InGaAs/InP Ring Oscillator Using Integrated Enhancement- and Depletion-Mode High-Electron Mobility Transistors

A. Mahajan, G. Cueva, M. Arafa, P. Fay, and I. Adesida

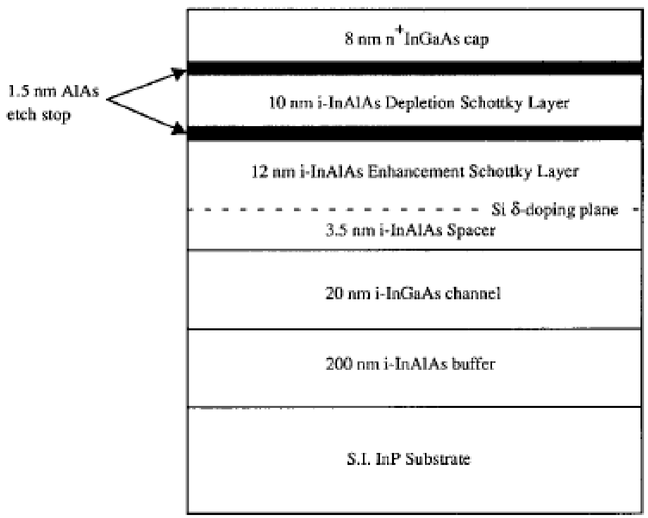

Fig. 1. Cross section diagram of MBE-grown layer structure used in this work.

Use of two etch stop layers to fabricate both E- and D-Mode transistors

Ring Oscillator

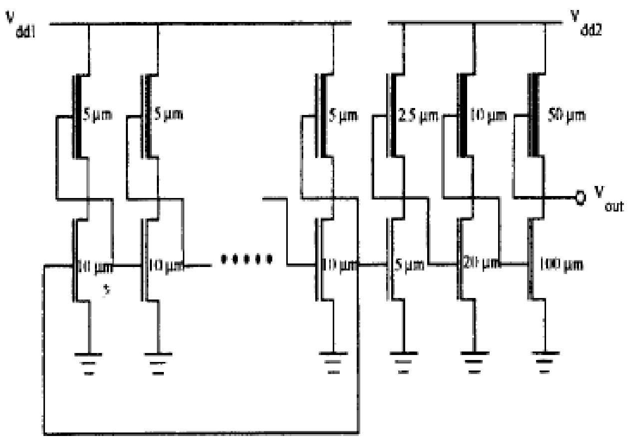

Fig. 6. Schematic for the ring oscillators.

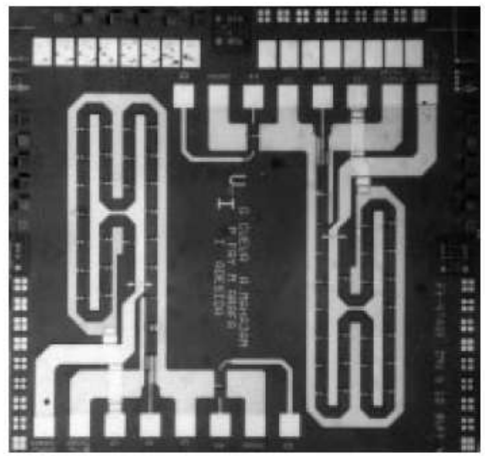

Fig. 7. Die photo of the completed 23 stage ring oscillator.

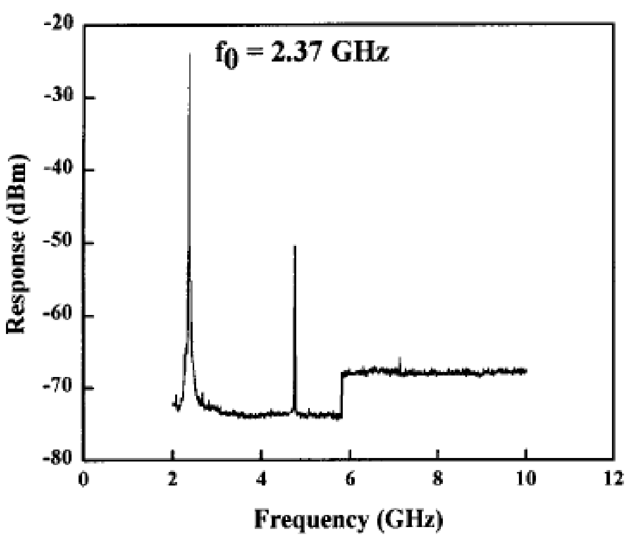

Fig. 8. Spectrum of output of 23 stage 0.25 µm gate-length ring oscillator with $V_{dd} = 0.4$ V.

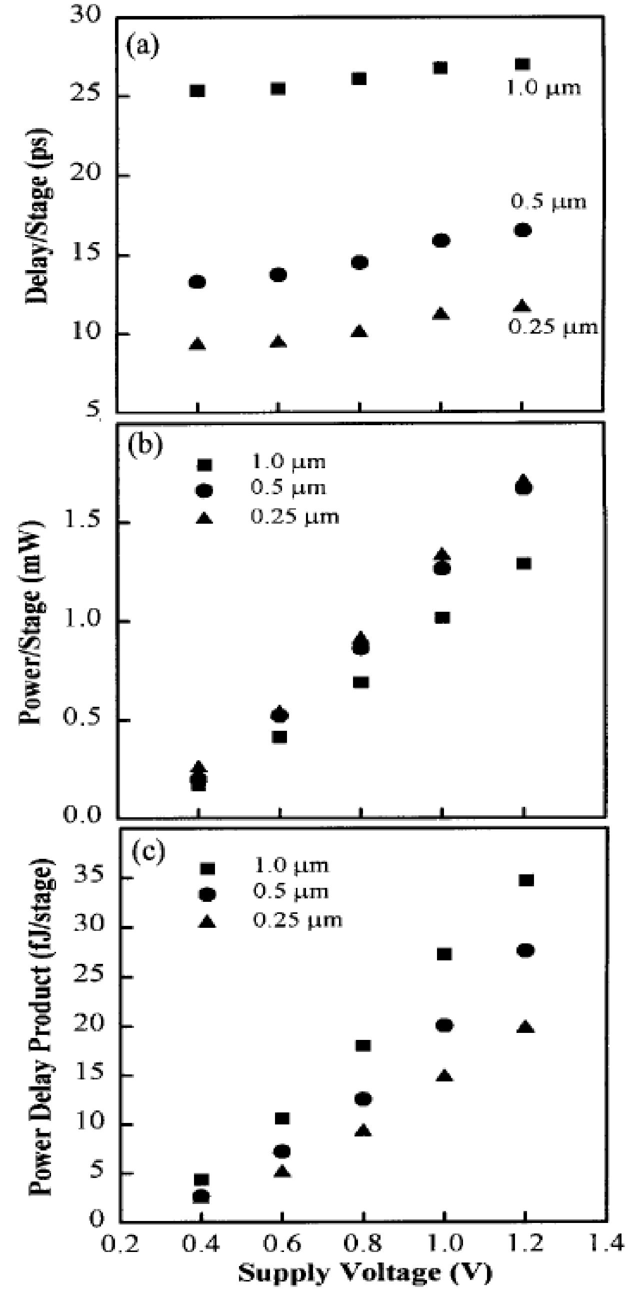

Fig. 9. (a) t_{pd}, (b) P_D and (c) PDP as a function of supply voltage for 1.0, 0.5 and 0.25 µm gate-length inverters.

Nanotechnology 4 (1993) 49–57. Printed in the UK

Quantum cellular automata

Craig S Lent, P Douglas Tougaw, Wolfgang Porod and Gary H Bernstein
Department of Electrical Engineering, University of Notre Dame, Notre Dame, IN 46556, USA

Received 1 August 1992, accepted for publication 24 December 1992

Pure Quantum Mechanics:

Quantum dots with diameter 10 nm
Nearest neighbor 20 nm

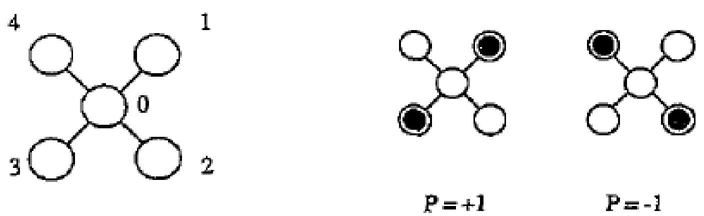

Figure 1. The quantum cell consisting of five quantum dots which are occupied by two electrons. The mutual Coulombic repulsion between the electrons results in bistability between the $P = +1$ and $P = -1$ states.

$$H_0^{\text{cell}} = \sum_{i,\sigma} E_{0,i} n_{i,\sigma} + \sum_{i,\sigma} t(a_{i,\sigma}^\dagger a_{0,\sigma} + a_{0,\sigma}^\dagger a_{i,\sigma}) + \sum_i E_Q n_{i,\uparrow} n_{i,\downarrow} + \sum_{i>j,\sigma,\sigma'} V_Q \frac{n_{i,\sigma} n_{j,\sigma'}}{|\boldsymbol{R}_i - \boldsymbol{R}_j|}. \quad (1)$$

$$(H_0^{\text{cell}} + H_{\text{inter}}^{\text{cell}})|\Psi_n\rangle = E_n|\Psi_n\rangle.$$

Switching behaviour

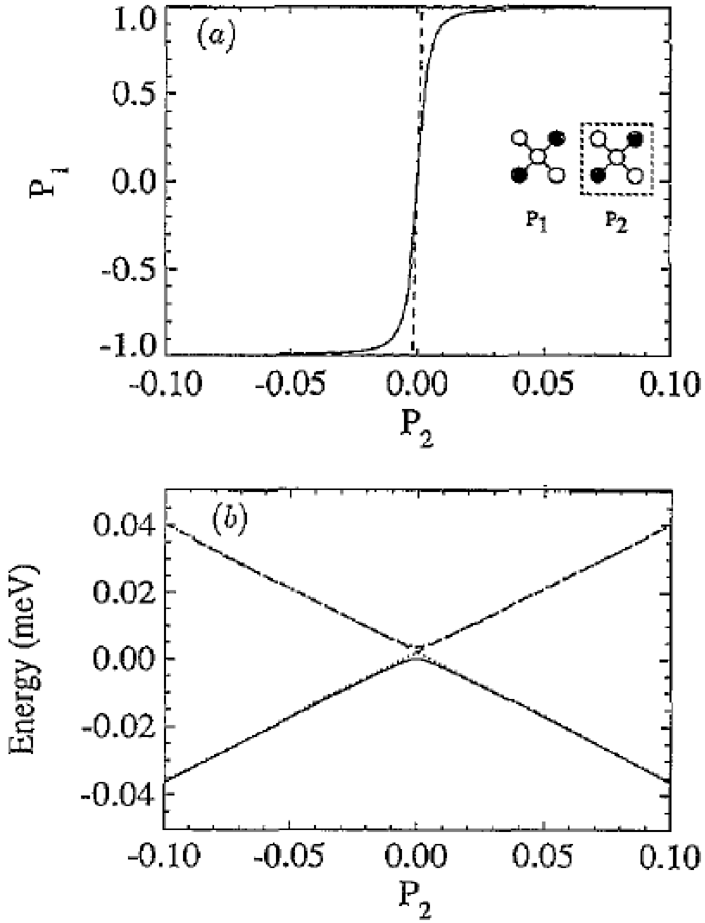

Figure 2. The cell–cell response function. The polarization of the right cell is fixed and the induced polarization in the left cell is calculated. (*a*) The calculated polarization of cell 1 as a function of the polarization of cell 2. Note that the range of P_2 shown is only from -0.1 to $+0.1$. This is because the transition in the induced polarization is so abrupt. (*b*) The first four eigen-energies of cell 1. The polarization of the lowest two are shown in (*a*).

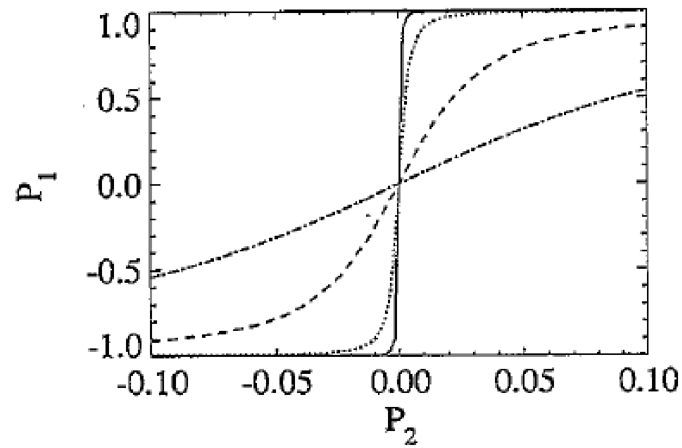

Figure 3. The cell–cell response function for various values of the dot-to-dot coupling energy (t in equation (1)). The induced cell polarization P_1 is plotted as a function of the neighboring cell polarization P_2. The results are shown for values of the coupling energy, $t = -0.2$ (full curve), -0.3 (dotted curve), -0.5 (dashed curve), and -0.7 (dot-dashed curve) meV. Note that the response is shown only for P_2 in the range $[-0.1, +0.1]$.

Edge driven computing

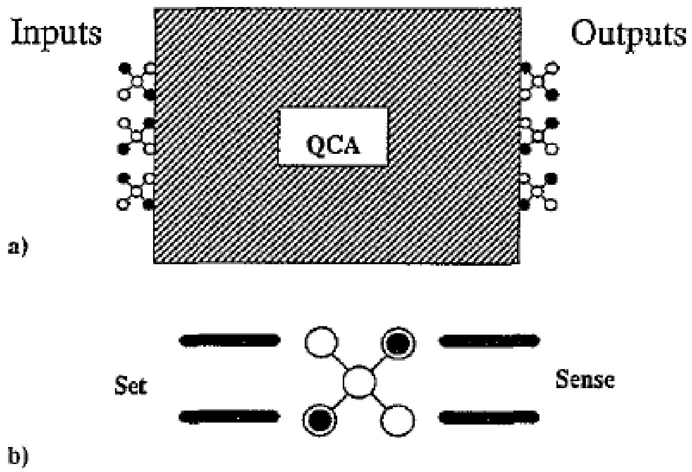

Figure 4. The new paradigm for computing with quantum cellular automata (QCAs). The input to the QCA is provided at an edge by setting the polarization state of the edge cells (*edge-driven computation*). The QCA is allowed to dissipatively move to its new ground-state configuration and the output is sensed at the other edge (*computing with the ground state*). The 'set' and 'sense' lines are shown schematically.

Transmission lines

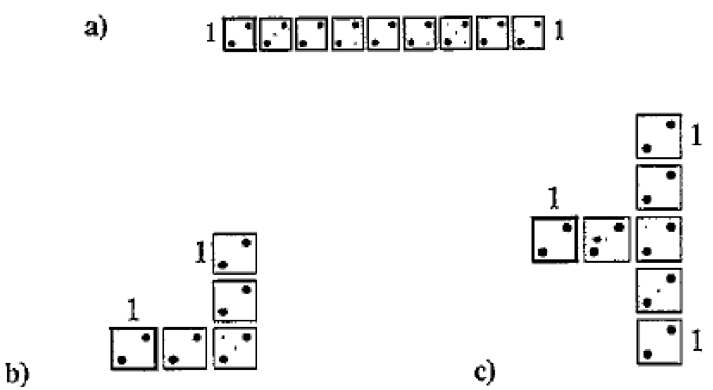

Figure 5. QCA wires: (*a*) the basic wire; (*b*) a corner in a wire; (*c*) fan-out of one signal into two channels. In each case the darker (left-hand) cell has a fixed polarization which constitutes the input. Note that these figures are not simply schematic, but are a plot of the results of a self-consistent many-body calculation of the ground state for the cellular array. The diameter of each circle is proportional to the calculated charge density at each site.

Circuits

Inverter

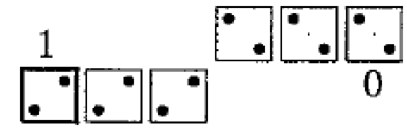

Figure 6. An inverter constructed from a quantum cell automaton.

OR gates

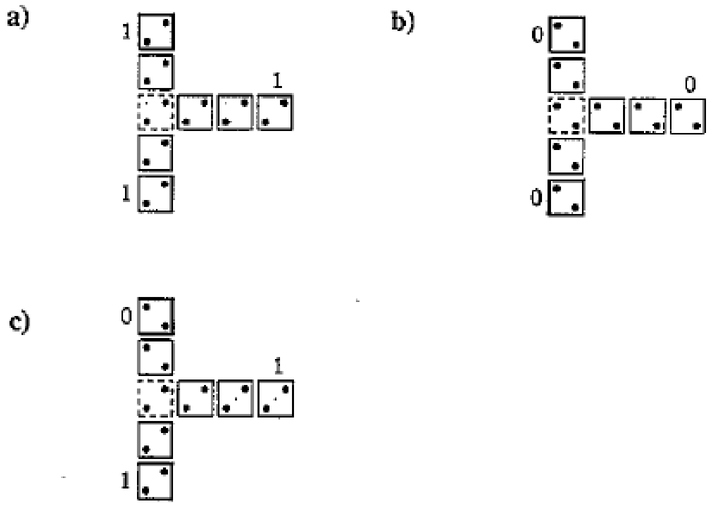

Figure 7. An OR gate. The cells in darker squares are fixed to the input states. The cell in the dashed square is biased slightly toward the '1' state.

AND gates

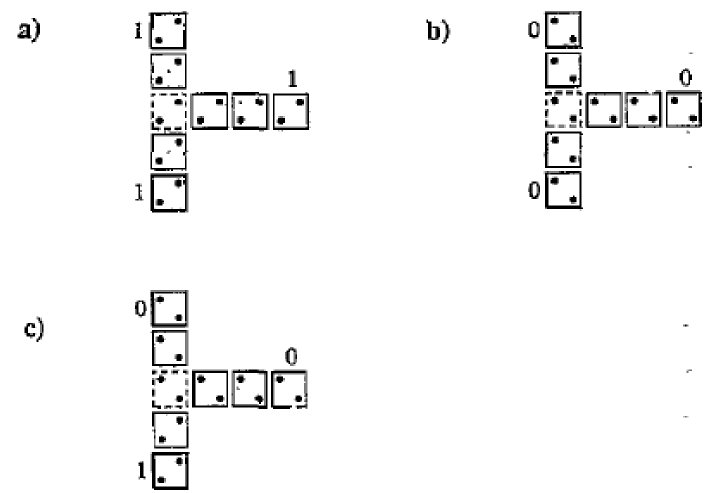

Figure 8. An AND gate. The cells in darker squares are fixed to the input states. The cell in the dashed square is biased slightly toward the '0' state.

Critical Issues and Benefits

Issues:

Uniform cell occupancy

Dot size control

Temperature

Benefits:

No interconnects

High density

Low power

Ultra-fast computing